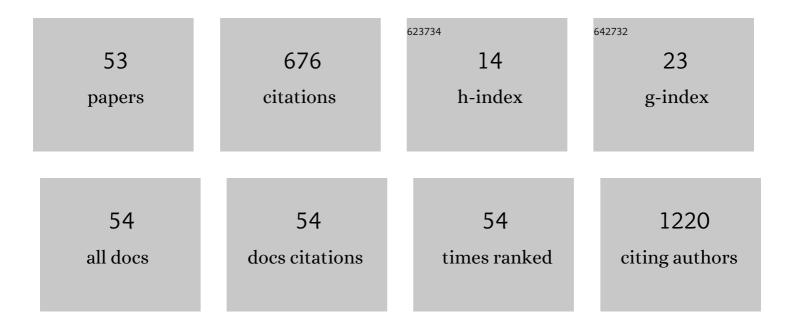
Johannes Boos

List of Publications by Year in descending order

Source: https://exaly.com/author-pdf/10986719/publications.pdf Version: 2024-02-01



#	Article	IF	CITATIONS
1	Diagnostic potential of PET/CT using a 68Ga-labelled prostate-specific membrane antigen ligand in whole-body staging of renal cell carcinoma: initial experience. European Journal of Nuclear Medicine and Molecular Imaging, 2017, 44, 102-107.	6.4	87
2	Prospective comparison of whole-body MRI and 68Ga-PSMA PET/CT for the detection of biochemical recurrence of prostate cancer after radical prostatectomy. European Journal of Nuclear Medicine and Molecular Imaging, 2019, 46, 1542-1550.	6.4	47
3	Prediction of outcome after aneurysmal subarachnoid haemorrhage using data from patient admission. European Radiology, 2018, 28, 4949-4958.	4.5	38
4	Does body mass index outperform body weight as a surrogate parameter in the calculation of size-specific dose estimates in adult body CT?. British Journal of Radiology, 2016, 89, 20150734.	2.2	34
5	CT pulmonary angiography: simultaneous low-pitch dual-source acquisition mode with 70 kVp and 40 ml of contrast medium and comparison with high-pitch spiral dual-source acquisition with automated tube potential selection. British Journal of Radiology, 2016, 89, 20151059.	2.2	28
6	Metal Artifact Reduction in Computed Tomography After Deep Brain Stimulation Electrode Placement Using Iterative Reconstructions. Investigative Radiology, 2017, 52, 18-22.	6.2	25
7	lterative metal artefact reduction (MAR) in postsurgical chest CT: comparison of three iMAR-algorithms. British Journal of Radiology, 2017, 90, 20160778.	2.2	24
8	Ovarian Cancer: Prevalence in Incidental Simple Adnexal Cysts Initially Identified in CT Examinations of the Abdomen and Pelvis. Radiology, 2018, 286, 196-204.	7.3	20
9	Dualâ€phase hybrid ¹⁸ Fâ€Fluoride Positron emission tomography/ <scp>MRI</scp> in ankylosing spondylitis: Investigating the link between <scp>MRI</scp> bone changes, regional hyperaemia and increased osteoblastic activity. Journal of Medical Imaging and Radiation Oncology, 2018, 62, 313-319.	1.8	18
10	MDCT vs. MRI for incidental pancreatic cysts: measurement variability and impact on clinical management. Abdominal Radiology, 2017, 42, 521-530.	2.1	17
11	ACCURACY OF SIZE-SPECIFIC DOSE ESTIMATE CALCULATION FROM CENTER SLICE IN COMPUTED TOMOGRAPHY. Radiation Protection Dosimetry, 2018, 178, 8-19.	0.8	17
12	Dual energy CT angiography: pros and cons of dual-energy metal artifact reduction algorithm in patients after endovascular aortic repair. Abdominal Radiology, 2017, 42, 749-758.	2.1	16
13	MRI identifies biochemical alterations of intervertebral discs in patients with low back pain and radiculopathy. European Radiology, 2019, 29, 6443-6446.	4.5	16
14	Biochemical imaging of cervical intervertebral discs with glycosaminoglycan chemical exchange saturation transfer magnetic resonance imaging: feasibility and initial results. Skeletal Radiology, 2016, 45, 79-85.	2.0	15
15	Performance and clinical impact of machine learning based lung nodule detection using vessel suppression in melanoma patients. Clinical Imaging, 2018, 52, 328-333.	1.5	15
16	Institutional computed tomography diagnostic reference levels based on water-equivalent diameter and size-specific dose estimates. Journal of Radiological Protection, 2018, 38, 536-548.	1.1	14
17	Fluoroscopic percutaneous brush cytology, forceps biopsy and both in tandem for diagnosis of malignant biliary obstruction. European Radiology, 2018, 28, 522-529.	4.5	14
18	Potential of a machine-learning model for dose optimization in CT quality assurance. European Radiology, 2019, 29, 3705-3713.	4.5	14

Johannes Boos

#	Article	IF	CITATIONS
19	Is CT-based cinematic rendering superior to volume rendering technique in the preoperative evaluation of multifragmentary intraarticular lower extremity fractures?. European Journal of Radiology, 2020, 126, 108911.	2.6	13
20	Low-tube voltage 100ÂkVp MDCT in screening of cocaine body packing: image quality and radiation dose compared to 120ÂkVp MDCT. Abdominal Imaging, 2015, 40, 2152-2158.	2.0	12
21	Electronic Kiosks for Patient Satisfaction Survey in Radiology. American Journal of Roentgenology, 2017, 208, 577-584.	2.2	12
22	Tailoring CT Dose to Patient Size. Academic Radiology, 2018, 25, 1624-1631.	2.5	12
23	Contrast-Enhanced Computed Tomography in Intensive Care Unit Patients with Acute Clinical Deterioration: Impact of Hyperattenuating Adrenal Glands. Canadian Association of Radiologists Journal, 2017, 68, 21-26.	2.0	11
24	Uterine Artery Embolization with Gelfoam for Acquired Symptomatic Uterine Arteriovenous Shunting. Journal of Vascular and Interventional Radiology, 2019, 30, 1750-1758.	0.5	11
25	CT Intensity Distribution Curve (Histogram) Analysis of Patients Undergoing Antiangiogenic Therapy for Metastatic Renal Cell Carcinoma. American Journal of Roentgenology, 2017, 209, W85-W92.	2.2	10
26	Evaluation of the impact of organ-specific dose reduction on image quality in pediatric chest computed tomography. Pediatric Radiology, 2014, 44, 1065-1069.	2.0	9
27	<scp>CT</scp> angiography of the aorta using 80 <scp>kVp</scp> in combination with sinogramâ€affirmed iterative reconstruction and automated tube current modulation: Effects on image quality and radiation dose. Journal of Medical Imaging and Radiation Oncology, 2016, 60, 187-193.	1.8	9
28	Impact of different metal artifact reduction techniques on attenuation correction in 18F-FDG PET/CT examinations. British Journal of Radiology, 2020, 93, 20190069.	2.2	9
29	Improvement of water saturation shift referencing by sequence and analysis optimization to enhance chemical exchange saturation transfer imaging. Magnetic Resonance Imaging, 2016, 34, 771-778.	1.8	8
30	Metal artifact reduction (MAR) based on two-compartment physical modeling: evaluation in patients with hip implants. Acta Radiologica, 2017, 58, 70-76.	1.1	8
31	Comparison of B0 versus B0 and B1 field inhomogeneity correction for glycosaminoglycan chemical exchange saturation transfer imaging. Magnetic Resonance Materials in Physics, Biology, and Medicine, 2018, 31, 645-651.	2.0	8
32	Diagnostic value of CT-localizer and axial low-dose computed tomography for the detection of drug body packing. Journal of Clinical Forensic and Legal Medicine, 2016, 37, 55-60.	1.0	7
33	Heparin-bonded stent graft treatment for major visceral arterial injury after upper abdominal surgery. European Radiology, 2018, 28, 3221-3227.	4.5	7
34	Adnexal mass staging CT with a disease-specific structured report compared to simple structured report. European Radiology, 2019, 29, 4851-4860.	4.5	7
35	Implementation of Institutional Size-Specific Diagnostic Reference Levels for CT Angiography. Academic Radiology, 2019, 26, 1661-1667.	2.5	7
36	Optimizing radiation exposure in screening of body packing: image quality and diagnostic acceptability of an 80 kVp protocol with automated tube current modulation. Forensic Science, Medicine, and Pathology, 2017, 13, 145-150.	1.4	6

Johannes Boos

#	Article	IF	CITATIONS
37	What Is the Optimal Abdominal Aortic Aneurysm Sac Measurement on CT Images during Follow-up after Endovascular Repair?. Radiology, 2017, 285, 1032-1041.	7.3	6
38	Split-Bolus Injection Producing Simultaneous Late Arterial and Portal Venous Phases in CT Enterography: Preliminary Results. American Journal of Roentgenology, 2017, 209, 1056-1063.	2.2	5
39	Diagnostic value and forensic relevance of a novel photorealistic 3D reconstruction technique in post-mortem CT. British Journal of Radiology, 2020, 93, 20200204.	2.2	5
40	Split-bolus intravenous contrast material injection vs. single-bolus injection in patients following endovascular abdominal aortic repair (EVAR). Abdominal Radiology, 2017, 42, 2551-2561.	2.1	4
41	Value of delayed gadolinium-enhanced magnetic resonance imaging of cartilage for the pre-operative assessment of cervical intervertebral discs. Journal of Orthopaedic Research, 2017, 35, 1824-1830.	2.3	4
42	Radiologists' Experience With Patient Interactions in the Era of Open Access of Patients to Radiology Reports. Journal of the American College of Radiology, 2018, 15, 1573-1579.	1.8	4
43	Age-related apparent diffusion coefficients of lumbar vertebrae in healthy children at 1.5 T. Pediatric Radiology, 2018, 48, 1008-1012.	2.0	3
44	Impact of different iterative metal artifact reduction (iMAR) algorithms on PET/CT attenuation correction after port implementation. European Journal of Radiology, 2020, 129, 109065.	2.6	3
45	Stent Lumen Visibility in Single-energy CT Angiography. Academic Radiology, 2016, 23, 752-759.	2.5	2
46	Diagnostic yield and clinical impact of microbiologic diagnosis from CT-guided drainage in patients previously treated with empiric antibiotics. Abdominal Radiology, 2017, 42, 298-305.	2.1	2
47	Comparison of glycosaminoglycan chemical exchange saturation transfer using Gaussianâ€shaped and offâ€resonant spinâ€lock radiofrequency pulses in intervertebral disks. Magnetic Resonance in Medicine, 2017, 78, 280-284.	3.0	2
48	Noise insertion in CT for cocaine body packing: where is the limit of extensive dose reduction?. European Journal of Medical Research, 2018, 23, 59.	2.2	1
49	Development of size-specific institutional diagnostic reference levels for computed tomography protocols in neck imaging. Journal of Radiological Protection, 2020, 40, 68-82.	1.1	1
50	Impact of increasing levels of adaptive statistical iterative reconstruction on image quality in oil-based postmortem CT angiography in coronary arteries. International Journal of Legal Medicine, 2021, 135, 1869-1878.	2.2	1
51	Impact of Different Metal Artifact Reduction Techniques on Attenuation Correction of Normal Organs in 18F-FDG-PET/CT. Diagnostics, 2022, 12, 375.	2.6	1
52	Observation time after outpatient non-arterial interventional procedures: standards, safety, and outcomes. Abdominal Radiology, 2017, 42, 1571-1578.	2.1	0
53	Typical doses and typical values for fluoroscopic diagnostic and interventional procedures. Journal of Radiological Protection, 2022, 42, 021510.	1.1	0